Oxyl and Hydroxyl Radical Transfer in Mitochondrial Amidoxime Reducing Component-Catalyzed Nitrite Reduction

Jing Yang,[†] Logan J. Giles,[†] Christian Ruppelt,[‡] Ralf R. Mendel,*[‡] Florian Bittner,*[‡] and Martin L. Kirk*[†]

[†]Department of Chemistry and Chemical Biology, The University of New Mexico, MSC03 2060, 1 University of New Mexico, Albuquerque, New Mexico 87131-0001, United States

[‡]Department of Plant Biology, Braunschweig University of Technology, Humboldtstrasse 1, 38023 Braunschweig, Germany

Ⓢ *Supporting Information*

ABSTRACT: A combination of electron paramagnetic resonance (EPR) spectroscopy and computational approaches has provided insight into the nature of the reaction coordinate for the one-electron reduction of nitrite by the mitochondrial amidoxime reducing component (mARC) enzyme. The results show that a paramagnetic Mo(V) species is generated when reduced enzyme is exposed to nitrite, and an analysis of the resulting EPR hyperfine parameters confirms that mARC is remarkably similar to the low-pH form of sulfite oxidase. Two mechanisms for nitrite reduction have been considered. The first shows a modest reaction barrier of 14 kcal/mol for the formation of ·NO from unprotonated nitrite substrate. In marked contrast, protonation of the substrate oxygen proximal to Mo in the Mo(IV)−O−N−O substrate-bound species results in barrierless conversion to products. A fragment orbital analysis reveals a high degree of Mo−O(H)−N−O covalency that provides a π-orbital pathway for one-electron transfer to the substrate and defines orbital constraints on the Mo−substrate geometry for productive catalysis in mARC and other pyranopterin molybdenum enzymes that catalyze this one-electron transformation.

Figure 1. Putative and experimentally derived structures for mARC in the Mo(IV), Mo(V), and Mo(VI) oxidation states.

The mitochondrial amidoxime reducing component (mARC) enzymes are members of the molybdenum cofactor (Moco) sulfurase C-terminal (MOSC) domain superfamily of pyranopterin Mo proteins.[1,2] The mARC enzymes (mARC-1 and mARC-2) possess a single MOSC/MOSC-N domain with Moco as the only redox chromophore. The first coordination sphere of the oxidized Mo site was recently revealed by extended X-ray absorption fine-structure (EXAFS) analysis, and the coordination geometry is depicted in Figure 1 along with putative structures of the reduced and Mo(V) enzyme forms.[3] The general active-site structures postulated for mARC enzymes (Figure 1) are similar to those of other sulfite oxidase (SO) family enzymes, where the oxidized form possesses a Mo(VI) ion coordinated by two terminal oxo ligands, a pyranopterin dithiolene (pdt) chelate, and a coordinated cysteine.

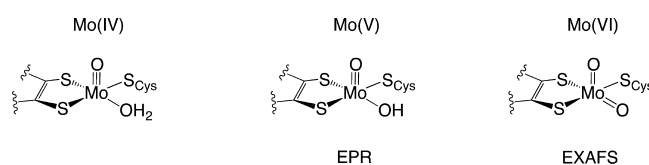The mARC enzyme possesses broad substrate specificity,[4−6] which is unusual for SO family enzymes. Amidoxime and N-hydroxylated guanidine prodrugs are readily absorbed in the gastrointestinal tract and reduced by mARC to their active forms.[6] Although the actual physiological substrates for mARC are not known, mARC can efficiently reduce N-hydroxycytosine to cytosine. This suggests a physiological role for mARC in the detoxification of base analogues that would otherwise be misincorporated into DNA with an increased frequency of mutations.[7] Human mARC has also been suggested to function as a regulator of intracellular ·NO concentrations since it can reduce N^4-hydroxy-L-arginine,[8] which is an intermediate in the conversion of L-arginine to NO by NO synthase. Remarkably, mARC has recently been shown to catalyze the reduction of nitrite ($NO_2^−$) to ·NO, indicating a potential biosynthetic pathway for ·NO production in humans.[9] This $NO_2^− \rightarrow$ ·NO conversion has also been observed for xanthine oxidase,[10] nitrate reductase,[11] and human SO.[12] Although mARC can catalyze transformations of a wide variety of substrates, the mechanistic details of these catalytic reductions and the electronic-structure basis for mARC reactivity are largely unknown. In general, the mechanistic details of one-electron catalysis, which is widely known for first-row transition metals in bioinorganic catalysis, are not understood for pyranopterin molybdenum enzymes. This results from the fact that these molybdenum enzymes are known to redox-cycle between a Mo(IV) site with a d^2 electron configuration and a two-electron-oxidized Mo(VI) center with a d^0 configuration.[13,14] The vast majority of two-electron catalytic transformations performed by pyranopterin molybdenum enzymes are coupled to the formal transfer of an oxygen atom between the Mo center and the substrate. Here we focus on the one-electron chemistry catalyzed by mARC in the reduction of $NO_2^−$ to ·NO.

Plant mARC isoform 2 (pmARC-2) from *Arabidopsis thaliana* (740 μM, phosphate buffer, pH 7.8, 300 mM NaCl)

was treated with an anaerobic solution containing 10× sodium dithionite and 50× NO_2^- in order to reduce the enzyme and initiate the catalytic reduction of NO_2^-. The procedure is similar to that used in prior enzyme studies showing that NO_2^-/dithionite elicits the evolution of ·NO.[9] It is well-known that nitrous acid (HNO_2) can disproportionate according to

$$3HNO_2 \rightleftharpoons H_3O^+ + NO_3^- + 2NO$$
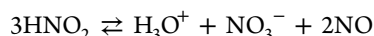
If mARC catalyzes the disproportionation of HNO_2, this would not involve net Mo redox cycling. However, the catalytic reduction of NO_2^- to ·NO is a one-electron reduction, and the reaction conditions employed[9] should result in a buildup of enzyme in the one-electron-oxidized paramagnetic Mo(V) state that is detectable by electron paramagnetic resonance (EPR) spectroscopy (Figure 1). After incubation with dithionite/nitrite for 10 min, a well-resolved EPR spectrum characteristic of the paramagnetic low-pH SO Mo(V) enzyme form arises (Figure 2). Spin quantitation of the signal shows nearly
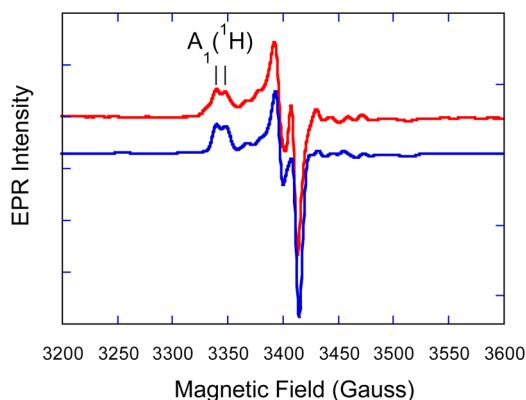

Figure 2. X-band (9.37 GHz, 77K) EPR spectrum of dithionite-reduced mARC in the presence of excess NO_2^- (red). The spectral simulation (blue) yielded the following spin Hamiltonian parameters: $g_{1,2,3}$ = 2.002, 1.967, 1.963; g_{ave} = 1.977; $A_{1,2,3}(^{95,97}Mo)$ = 168, 70, 60 MHz (Euler angles $\alpha = 0°$, $\beta = 16°$, $\gamma = 0°$); $A_{ave}(^{95,97}Mo)$ = 99 MHz; $A_{1,2,3}(^1H)$ = 26, 40, 20 MHz (Euler angles $\alpha = 0°$, $\beta = 0°$, $\gamma = 0°$); $A_{ave}(^1H)$ = 28.7 MHz. The $I = \frac{1}{2}$ ^1H splitting of g_1 (3344 G) is highlighted.

quantitative conversion to the Mo(V) species (76%). Although the EPR spectra of pmARC and low-pH forms of SO are similar, pmARC-2 does not possess the SO (SUOX) fold,[15] indicating that there are distinct differences between mARC and other SO family enzymes. This EPR spectrum is identical to that generated using human mARC that was partially reduced with NADH/cyt b5R/cyt b5.[16,17] To our knowledge this is the first report of the $^{95,97}Mo$ hyperfine anisotropy for the mARC Mo(V) enzyme form. The combined nature of the $^{95,97}Mo$ hyperfine tensor and the **g** tensor clearly indicates that the Mo(V) form of the enzyme is a monooxo species in which the single unpaired electron occupies a Mo(xy) redox orbital that is oriented orthogonal to the Mo≡O bond.[18−20] Thus, the observation of a Mo(V) EPR signal under these conditions provides strong evidence for the mARC-catalyzed one-electron reduction of nitrite to ·NO, allowing an investigation of the reaction coordinate and the nature of the frontier molecular orbitals in order to assess symmetry-restricted substrate binding at the Mo center and orbital control of the one-electron-transfer chemistry.

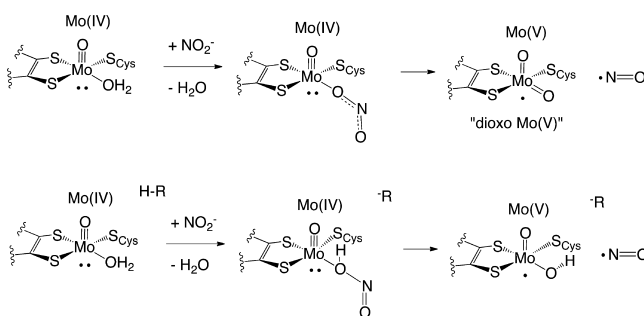In Figure 3, we show putative mechanisms for the mARC-catalyzed formation of ·NO from nitrite. The EPR spectrum

Figure 3. (top) Oxyl radical transfer mechanism and (bottom) hydroxyl radical transfer mechanism for the mARC-catalyzed formation of ·NO from NO_2^-. HR is a general acid that protonates the coordinated NO_2^-.

generated under the reaction conditions clearly shows evidence for strong coupling to a proton, indicating that the Mo(V) species that accumulates under turnover conditions is an oxomolybdenum $(pdt)MoO(SR_{Cys})(OH)$ site and not a dioxomolybdenum $(pdt)MoO_2(SR_{Cys})$ site. The observation of an equatorial hydroxyl proton (i.e., the protonated equatorial oxo) supports a mechanism involving one-electron reduction of the substrate that is coupled with a protonation step. More importantly, however, this leads to the question of exactly when this proton enters into the reaction sequence.

The reaction coordinate for mARC-catalyzed NO_2^- reduction was investigated using a combination of closed-shell singlet, open-shell broken-symmetry singlet, and spin triplet calculations using density functional theory.[21,22] The computed reaction coordinate for the oxyl radical transfer is depicted in Figure 4 (top). Although the computed reaction barrier ($\Delta H^{\ddagger}$) for oxyl radical transfer is only 14 kcal/mol, the reaction is essentially thermoneutral. This is the case because the Mo(V) dioxo species is inherently unstable toward protonation.[23] Thus, protonation of the $(pdt)MoO_2(SR_{Cys})$ equatorial oxo will contribute to an increase in the overall exergonic nature of the reaction. In contrast, protonation of the O_α oxygen of NO_2^- that is bound to the Mo(IV) ion leads to a hydroxyl radical transfer and barrierless conversion to the $(pdt)Mo^VO(SR_{Cys})$-(OH) and ·NO products (Figure 4, bottom). Interestingly, substrate protonation leads to an electronic structure that approximates the transition state for the conversion of the nonprotonated substrate to products. This occurs through polarization of the NO_2^- bonds (i.e., H−O−N≡O; Figure 3, bottom) and weakening of the N−O bond that is proximal to the Mo ion. In the spin-unrestricted broken-symmetry approximation, this results in a large exchange splitting of the Mo(xy) α (↑) and β (↓) spin orbitals (Figure 5, left). This large exchange splitting results in a strong polarization of the Mo(xy) α (↑) and β (↓) spin orbitals that energetically drives a $Mo^{IV} \rightarrow HNO_2$ one-electron transfer to yield $(pdt)Mo^VO(SR_{Cys})(OH)$ and ·NO.

The fragment orbital analysis[21,22] of the spin-unrestricted broken-symmetry calculation reveals the key donor−acceptor orbital interactions that result in the barrierless conversion to product. Specifically, the spin-down β (↓) electron originally localized in the highest occupied molecular orbital (HOMO) of the Mo(IV) fragment has been delocalized onto the lowest unoccupied molecular orbital (LUMO) of the HNO_2 substrate.
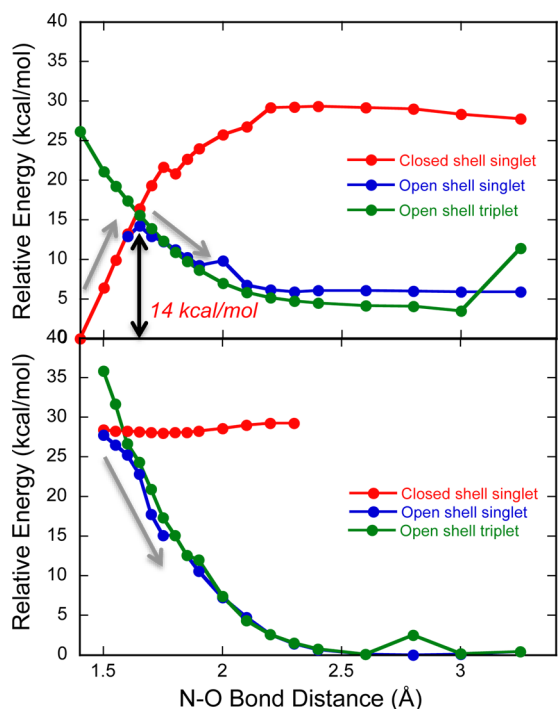
Figure 4. Reaction coordinates for (top) oxyl and (bottom) hydroxyl radical transfer. It should be noted that in the hydroxyl case (bottom panel) the reaction proceeds smoothly from high energy (Mo(IV) + substrate) to low energy (Mo(V) + product) without going over a transition state barrier.
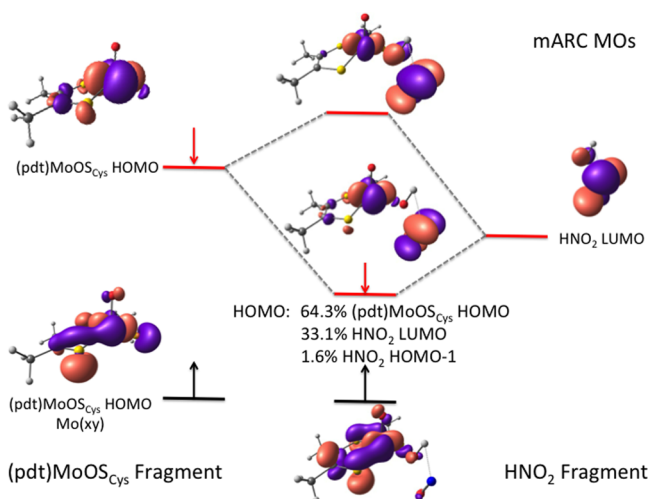

Figure 5. Spin-unrestricted broken-symmetry description of mARC-catalyzed N−O bond cleavage for r_{N-O} = 1.5 Å (α spin orbitals are shown in black and β spin orbitals in red). The delocalization of the (pdt)MoOS$_{Cys}$ β ($\downarrow$) electron (red arrow) into the HNO$_2$ LUMO should be noted. There is a large spin polarization in the broken-symmetry mARC frontier MOs, with the β ($\downarrow$) HOMO possessing Mo(xy) and ·NO π^* character and the α ($\uparrow$) HOMO possessing Mo(xy) and essentially no ·NO π^* character. The description is similar for the transition state using NO$_2^-$ as the substrate (r_{N-O} = 1.7 Å). In the calculations, the pdt was modeled as [C$_4$H$_6$S$_2$]$^{2-}$, and S$_{Cys}$ as [C$_2$H$_5$S]$^{1-}$.

The HNO$_2$ fragment β LUMO (Figure 5, right) now comprises a significant portion of the "reactant" MO with appreciable diatomic ·NO product π^* character. This orbital description is essentially identical to that obtained at the transition state for the conversion of unprotonated NO$_2^-$ to ·NO. Importantly, it is the Mo−substrate d−p π interaction that is key to providing a highly efficient pathway for the Mo(IV) → HNO$_2$ single-electron transfer. The fact that the Mo(xy) redox orbital is oriented orthogonal to the Mo≡O bond allows one to postulate that the catalytically productive geometry for NO$_2^-$ reduction must be one in which the Mo≡O bond is oriented in the same plane as the (H)O−N−O atoms of the substrate (Figure 3).

In conclusion, the observation of barrierless one-electron transfer between Mo(IV) and HNO$_2$ and conversion to products favors a hydroxyl radical transfer mechanism for mARC upon substrate protonation. Oxyl radical transfer occurs with a modest reaction barrier (14 kcal/mol) when the substrate is not protonated. Thus, a picture begins to emerge wherein mARC is a SO-type protein that can catalyze both two-electron (e.g., amidoxime) and one-electron (NO$_2^-$) substrate reductions. The latter requires a key α-protonation step to facilitate homolytic N−O bond scission and barrierless hydroxyl radical transfer to Mo. The frontier orbital analysis of the reaction coordinate also defines key aspects of substrate attack relative to the active-site geometry.

■ ASSOCIATED CONTENT

Ⓢ Supporting Information

Experimental and computational details and complete ref 21 (as SI ref 3). This material is available free of charge via the Internet at http://pubs.acs.org.

■ AUTHOR INFORMATION

Corresponding Authors

*mkirk@unm.edu
*f.bittner@tu-bs.de
*r.mendel@tu-bs.de

Notes

The authors declare no competing financial interest.

■ ACKNOWLEDGMENTS

■ REFERENCES

(1) Anantharaman, V.; Aravind, L. *FEMS Microbiol. Lett.* **2002**, *207*, 55.
(2) Ott, G.; Havemeyer, A.; Clement, B. *J. Biol. Inorg. Chem.* **2015**, *20*, 265.
(3) Giles, L. J.; Ruppelt, C.; Yang, J.; Mendel, R. R.; Bittner, F.; Kirk, M. L. *Inorg. Chem.* **2014**, *53*, 9460.
(4) Havemeyer, A.; Grunewald, S.; Wahl, B.; Bittner, F.; Mendel, R.; Erdelyi, P.; Fischer, J.; Clement, B. *Drug Metab. Dispos.* **2010**, *38*, 1917.
(5) Havemeyer, A.; Bittner, F.; Wollers, S.; Mendel, R.; Kunze, T.; Clement, B. *J. Biol. Chem.* **2006**, *281*, 34796.
(6) Gruenewald, S.; Wahl, B.; Bittner, F.; Hungeling, H.; Kanzow, S.; Kotthaus, J.; Schwering, U.; Mendel, R. R.; Clement, B. *J. Med. Chem.* **2008**, *51*, 8173.
(7) Krompholz, N.; Krischkowski, C.; Reichmann, D.; Garbe-Schönberg, D.; Mendel, R. R.; Bittner, F.; Clement, B.; Havemeyer, A. *Chem. Res. Toxicol.* **2012**, *25*, 2443−2450.
(8) Kotthaus, J.; Wahl, B.; Havemeyer, A.; Kotthaus, J.; Schade, D.; Garbe-Schönberg, D.; Mendel, R.; Bittner, F.; Clement, B. *Biochem. J.* **2011**, *433*, 383.

(9) Sparacino-Watkins, C. E.; Tejero, J.; Sun, B.; Gauthier, M. C.; Thomas, J.; Ragireddy, V.; Merchant, B. A.; Wang, J.; Azarov, I.; Basu, P.; Gladwin, M. T. *J. Biol. Chem.* **2014**, *289*, 10345.

(10) Maia, L. B.; Moura, J. J. G. *J. Biol. Inorg. Chem.* **2011**, *16*, 443.

(11) Rockel, P.; Strube, F.; Rockel, A.; Wildt, J.; Kaiser, W. M. *J. Exp. Bot.* **2002**, *53*, 103−110.

(12) Wang, J.; Krizowski, S.; Fischer-Schrader, K.; Niks, D.; Tejero, J.; Sparacino-Watkins, C.; Wang, L.; Ragireddy, V.; Frizzell, S.; Kelley, E. E.; Zhang, Y.; Basu, P.; Hille, R.; Schwarz, G.; Gladwin, M. T. *Antioxid. Redox Signaling* **2014**, DOI: 10.1089/ars.2013.5397.

(13) Hille, R.; Hall, J.; Basu, P. *Chem. Rev.* **2014**, *114*, 3963.

(14) Kirk, M. L.; Stein, B. In *Comprehensive Inorganic Chemistry II*, 2nd ed.; Reedijk, J., Poeppelmeier, K., Eds.; Elsevier: Amsterdam, 2013; Vol. 3, p 263.

(15) Workun, G. J.; Moquin, K.; Rothery, R. A.; Weiner, J. H. *Microbiol. Mol. Biol. Rev.* **2008**, *72*, 228.

(16) Astashkin, A. V.; Hood, B. L.; Feng, C. J.; Hille, R.; Mendel, R. R.; Raitsimring, A. M.; Enemark, J. H. *Biochemistry* **2005**, *44*, 13274.

(17) Wahl, B.; Reichmann, D.; Niks, D.; Krompholz, N.; Havemeyer, A.; Clement, B.; Messerschmidt, T.; Rothkegel, M.; Biester, H.; Hille, R.; Mendel, R. R.; Bittner, F. *J. Biol. Chem.* **2010**, *285*, 37847.

(18) Yang, J.; Rothery, R.; Sempombe, J.; Weiner, J. H.; Kirk, M. L. *J. Am. Chem. Soc.* **2009**, *131*, 15612.

(19) Drew, S. C.; Hill, J. P.; Lane, I.; Hanson, G. R.; Gable, R. W.; Young, C. G. *Inorg. Chem.* **2007**, *46*, 2373.

(20) Drew, S. C.; Young, C. G.; Hanson, G. R. *Inorg. Chem.* **2007**, *46*, 2388.

(21) Frisch, M. J.; et al. *Gaussian 09*; Gaussian, Inc.: Wallingford, CT, 2009.

(22) Molecular orbitals were analyzed using the AOMix program. See: (a) Gorelsky, S. I. *AOMix: Program for Molecular Orbital Analysis*; York University: Toronto, 1997; http://www.sg-chem.net/aomix/. (b) Gorelsky, S. I.; Lever, A. B. P. *J. Organomet. Chem.* **2001**, *635*, 187−196.

(23) Xiao, Z. G.; Gable, R. W.; Wedd, A. G.; Young, C. G. *J. Am. Chem. Soc.* **1996**, *118*, 2912.